THE JOURNAL OF PHYSICAL CHEMISTRY B

ARTICLE

pubs.acs.org/JPCB

Elongation of the Fe—His Bond in the α Subunit Induced by Binding of the Allosteric Effector Bezafibrate to Hemoglobins

Shigenori Nagatomo,*[,†] Hiromi Hamada,[‡] and Hiroyuki Yoshikawa[‡]

[†]Department of Chemistry, University of Tsukuba, Tsukuba, Ibaraki 305-8571, Japan

[‡]Department of Obstetrics and Gynecology, Institute of Clinical Medicine, University of Tsukuba, Tsukuba, Ibaraki 305-8575, Japan

Supporting Information

ABSTRACT: Human adult hemoglobin (HbA), possessing an $\alpha_2\beta_2$ tetramer structure, efficiently transports oxygen from the lungs to the tissues. The oxygen affinity of HbA has been shown to be regulated by organic phosphates such as 2,3-bisphosphoglycerate (BPG). Bezafibrate (BZF) is also known to alter the oxygen affinity of HbA through a mechanism largely different from that of BPG. The interaction of HbA with BZF has been characterized by ^{1}H NMR to elucidate the molecular mechanism responsible for the functional alteration of HbA. Paramagnetically shifted heme methyl proton signals of only the α subunit of met-azido HbA exhibited sizable downfield shifts in the presence of BZF. Since met-azido HbA exhibits the so-called thermal spin equilibrium between high and low spin states, the BZF-induced shift changes observed for the α signals can be attributed to an increase in the high spin contents in the subunit, possibly due to the elongation of the Fe—His bond.

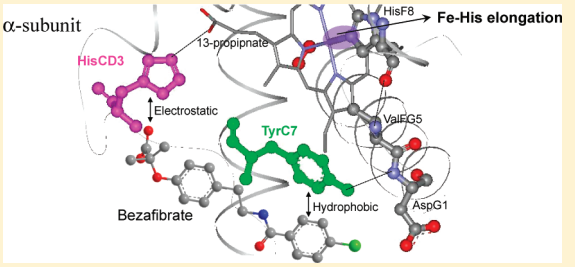

INTRODUCTION

Human adult hemoglobin (HbA) possessing an $\alpha_2\beta_2$ tetramer structure efficiently transports oxygen from the lungs to the tissues, exhibiting cooperativity in oxygen binding. Thus, it has been recognized as an important and basic model for allosteric proteins[1] and elucidation of a structural mechanism for cooperativity has been a major subject in Hb studies. Regulation of the oxygen affinity of HbA has been shown to be carried out by allosteric effectors such as H^+, Cl^-, 2,3-bisphosphoglycerate (BPG) and inositol(hexakis)phosphate (IHP).[2,3] BPG and IHP bind to the deoxy form of HbA and reduce the oxygen affinity of deoxy HbA. X-ray crystallographic studies have demonstrated the presence of two distinct quaternary structures, called T (tense) and R (relaxed) states, which correspond to the low- and high-O_2 affinity forms of the protein, respectively. Their typical structures are observed for the deoxy and CO (carbon monoxide)—bound forms of HbA, respectively.[4,5] The cooperative oxygen binding of HbA has been explained in terms of a reversible transition between the two quaternary structures.[6−8]

However, recent and more extensive examinations of HbA at a wide range of pH in the presence of the allosteric effector bezafibrate (BZF) (see Figure 1a), showed a reduction of the oxygen affinity of oxy HbA and stressed the importance of the tertiary structure change for oxygen affinity.[9−13] Thus, the effect of BZF is different from those of organic phosphates such as BPG and IHP.[10]

X-ray analysis of horse carbonmonoxy hemoglobin, to which BZF is bound and which adopts the R structure, as found by Shibayama et al., clarified that BZF binds to the globin near the E-helix of the α subunit, which is distinct from the binding of BPG and IHP to the central cavity at an intersubunit space between the two β subunits.[14] The BZF binding to the fully liganded form may cause tertiary structure change within the R structure, and therefore not only quaternary structure change but also the tertiary structure change may be responsible for the decrease of oxygen affinity and the low cooperativity.

So far there have been many reports that indicate the importance of tertiary structure to functions of HbA.[15−25] Friedman et al. report that differences of geminate recombination within T-, and R-quaternary structures are linked to Fe—His frequency observed in stable deoxy species or transient deoxy species.[15−17,20,21,23] These are examples in which tertiary structure change near the heme without quaternary structure change influences function (= geminate recombination).[15−17,20,21,23] Furthermore, Friedman et al. report that quaternary T structure can accommodate a range of tertiary structures; from the crystallographically well-defined deoxy T state (low-affinity) to the loosened T state constraints.[22,24,25] This suggests that quaternary T structure which adopts a range of tertiary structures keeps the extent of values about functions such as ligand reactivity and geminate recombination.[22,24,25]

Thus, it has been suggested that the binding of BZF to HbA induces the elongation of the Fe—His bond, which is closely related to tertiary structure change.[26] In a previous resonance

Received: May 29, 2011
Revised: September 29, 2011
Published: September 29, 2011

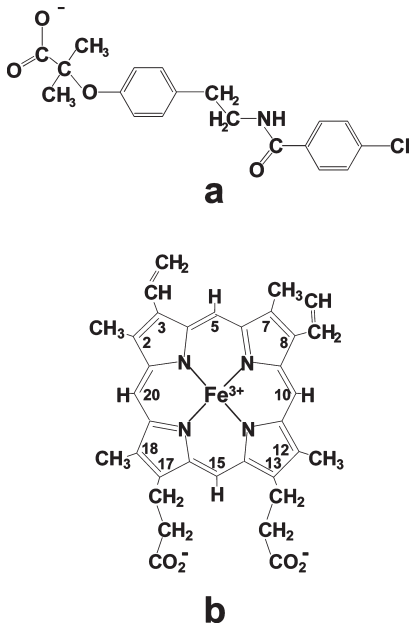

Figure 1. The molecular structure of bezafibrate (BZF) (a). The molecular structure and numbering of iron protoporphyrin IX (protoheme) (b).

Raman study, Nagatomo et al. observed Fe−His frequency after 10 ps CO photodissociation of carbonmonoxy Hb (COHb) with or without BZF.[26,27] Here, Fe−His is the bond between the heme iron atom (Figure 1b) and the proximal histidine (HisF8). The observed Fe−His frequency is 231 cm^{-1} and 229 cm^{-1} in the absence and presence, respectively, of BZF.[26] The Fe−His frequency at 10 ps after photolysis is believed to reflect some properties of the CO-bound form, considering that the shift of the Fe−His frequency for COHb takes place with a time constant of ∼300 ps.[28] Friedman et al. report that Fe−His frequencies after 8 ns CO photodissociation of COHb decrease in the presence of allosteric effectors.[21−25] The frequency difference between the absence and presence of BZF, therefore, strongly suggests the elongation of the Fe−His bond in the presence of BZF.[26] However, in this resonance Raman experiment, we do not know whether the elongation of the Fe−His bond is in the α or β subunit.

To investigate the properties of the Fe−His bond in the presence of BZF in detail, we analyzed the influence of Fe−His bond induced by BZF binding to the fully liganded form through ^{1}H NMR. In particular, we focused on the met-azido form. The met-azido derivatives of heme proteins in general share a certain property—they exhibit a thermal equilibrium between the high spin, $S = 5/2$, and low spin, $S = 1/2$, state due to the intermediate ligand field strength of the azido ligand.[29−32] Hence, changes in the population of the two spin states in equilibrium provide a sensitive probe of the effective axial field strength. Moreover, since both met-azido form and COHb, which are fully liganded forms, adopt the R quaternary structure,[33] ^{1}H NMR measurements of the met-azido form may enable us to estimate the influence of the Fe−His bond induced by BZF binding to fully liganded forms.

In this paper, we discuss the change of the Fe−His bond, which is closely related to tertiary structure change, induced by BZF binding to fully liganded forms. The present study demonstrates that BZF binding to fully liganded forms causes the elongation of the Fe−His bond in the α subunit. It is suggested that the elongation of the Fe−His bond, which causes not only quaternary structure change, but also tertiary structure change is important in the regulation of oxygen affinity.

EXPERIMENTAL SECTION

Materials. HbA was prepared from blood obtained from the Medical Center at the University of Tsukuba using the reported procedure.[34] Human fetal hemoglobin (HbF) possessing $\alpha_2\gamma_2$ tetramer structure was isolated and purified in the carbonmonoxy form from blood withdrawn from the cord of a patient, who agreed to the donation, in the Medical Center according to the method previously described.[35] Met-aquo Hb was prepared from carbonmonoxy Hb under a stream of oxygen with strong illumination in the presence of 5-fold molar excess of potassium ferricyanide (Wako Chemical Co.). The protein was separated from the residual chemicals using a Sephadex G-50 (Sigma Chemical Co.) column equilibrated with 50 mM Bis-Tris (Sigma Chemical Co.), pH 6.5. Met-azido Hb was prepared by the addition of 10-fold molar excess of sodium azido (Wako Chemical Co.) to met-aquo Hb. The Hb solution was concentrated to about 0.25 mM and the solvent was exchanged to ^2H_2O in an ultrafiltration cell (Amicon). BZF (Sigma Chemical Co.) was dissolved in the phosphate buffer at pH 8.0 and was added to the Hb solution. The pH of the sample was adjusted using 0.2 M NaOH or 0.2 M HCl, and the value was measured using an Horiba F-22 pH meter equipped with a Horiba type 6069−10D electrode.

Methods. NMR spectra were recorded with a Bruker AVANCE-400 FT NMR spectrometer operating at the ^{1}H frequency of 400 MHz. The spectra were obtained with about 3k transients, a spectral width of 20 kHz, 16k data points, a 10.2 μs 90° pulse, and a recycle time of 0.5 s. Chemical shifts are given in ppm downfield from sodium 2,2-dimethyl-2-silapentane-5-sulfonate with the residual H^2HO as an internal reference.

RESULTS

BZF Concentration Dependence of Paramagnetically Shifted ^{1}H NMR Spectra of met-azido HbA and HbF. We first analyzed the effects of BZF addition on the heme electronic structure of met-azido HbA and HbF using ^{1}H NMR spectra to estimate the strength of the axial ligand fields of the heme iron atom. It is known that the axial ligand field of the heme iron atom in the ferric state is reflected sensitively in the heme electronic structure.[29]

The low-field portion of the 400 MHz ^{1}H NMR spectrum of met-azido HbA at 45 °C is illustrated in spectrum a of Figure 2, in which six heme methyl proton resonances are resolved below 14 ppm and are assigned as indicated in the spectrum,[30,31] and similar spectra were observed in HbF.[32] Thus, paramagnetic ^{1}H NMR spectra of met-azido HbA and HbF enable us to discriminate and analyze each subunit.

The low-field portion of the 400 MHz ^{1}H NMR spectra of met-azido HbA in the presence of different concentrations of BZF at 45 °C is illustrated in spectra b, c, d, and e of Figure 2. With increasing concentration of BZF ([BZF]), the heme methyl proton signals for the met-azido form in the α subunit exhibited progressive downfield shifts, while small signal shifts in the β subunit were observed. In the low-field portion of the 400 MHz ^{1}H NMR spectra of met-azido HbF, a similar result was obtained:

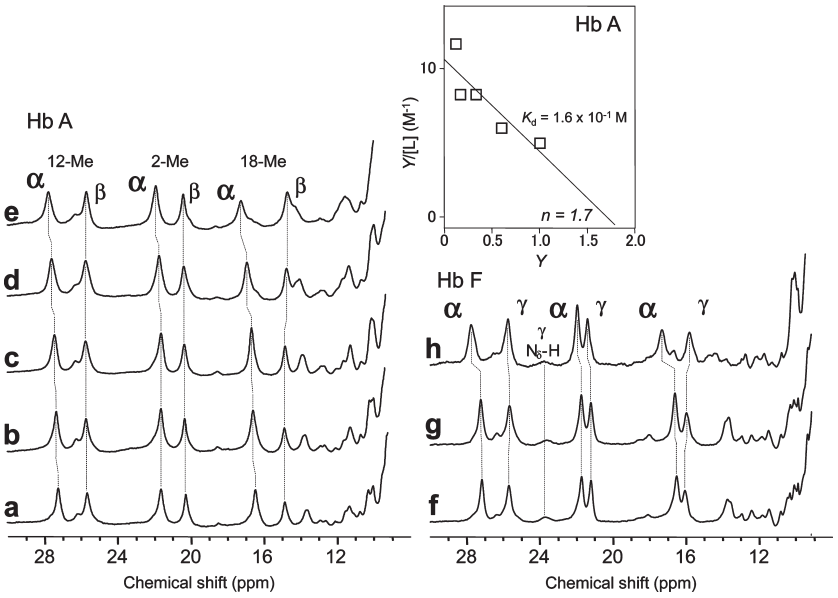

Figure 2. 400 MHz ^{1}H NMR spectra of met-azido HbA at pH 7.0 at 45 °C in the absence of BZF (a) and in the presence of [BZF]/[heme] of 10 (b), 20 (c), 40 (d), and 100 (e) and of met-azido HbF at pH 7.0 at 45 °C in the absence of BZF (f) and in the presence of [BZF]/[heme] of 10 (g) and 100 (h). (inset) The binding constant and stoichiometry calculated from the 18-Me signal in the α subunit in the binding of BZF to HbA according to Scatchard analysis.

with the BZF addition, the heme methyl proton signals for the met-azido form in the α subunit and the γ subunit exhibited progressive downfield shifts and small signal shifts, respectively. Comparisons of e with a in HbA and of h with f in HbF in Figure 2 suggest that BZF interacts with the α subunit to influence the electronic structure of heme in the α subunit, but not in the β and γ subunits.

BZF addition ([BZF]/[heme] = 100; here, [BZF]/[heme] represents the concentration ratio between heme and BZF) to met-azido HbA caused downfield shifts of the 12-Me peak of 27.23 ppm by 0.55 ppm, the 2-Me peaks of 21.64 ppm by 0.29 ppm, and the 18-Me peaks of 16.50 ppm by 0.79 ppm. BZF addition ([BZF]/[heme] = 100) to met-azido HbF also caused downfield shifts of the 12-Me peak of 27.17 ppm by 0.60 ppm, the 2-Me peaks of 21.73 ppm by 0.23 ppm, and the 18-Me peaks of 16.53 ppm by 0.81 ppm similar to the case of met-azido HbA. Proximal HisF8 N_δ-H proton of the γ subunit was observed at 23.30 ppm, and the chemical shift of this peak did not exhibit BZF dependence. Moreover, BZF addition ([BZF]/[heme] = 100) to met-azido HbA and HbF caused some broadening of heme methyl proton signals in the α subunit.

Thus, the preferential binding of BZF to the α subunit in HbA and HbF is apparent; this result is consistent with earlier findings.[14]

Stoichiometry of HbA with BZF. Next, we determined the stoichiometry and dissociation constant of HbA with an allosteric effector, namely, BZF, from the analysis of paramagnetically shifted heme methyl proton signals, because it is difficult to discriminate the change of the α or β subunit in the analysis of the UV−visible spectra change of HbA caused by BZF addition.

We again focus on the low-field portion of the 400 MHz ^{1}H NMR spectrum of met-azido HbA in the presence of varying concentrations of BZF, illustrated in spectrum b, c, d, and e of Figure 2. As discussed in a previous section, the downfield shifts of heme methyl proton signals for the met-azido form were observed in the α subunit only. When [BZF]/[heme] was 100, we assumed that the BZF binding to met-azido HbA was entirely complete, and we estimated the stoichiometry of HbA with BZF through Scatchard analysis of the data of met-azido HbA shown in Figure 2.

Scatchard plots of 18-Me proton signals of the α subunit are shown in the inset of Figure 2. The plots could be satisfactorily represented as a straight line; they gave a dissociation constant (K_d) of 1.6 × 10^{-1} M and a number of binding sites (n) of 1.7. These values seem to be consistent with the values (n = 2; K_d = 4 × 10^{-2} M[36] and n = 2; K_d = 1.5 × 10^{-1} M[37]) obtained from previous UV−vis experiments, considering that the dissociation constant between HbA and allosteric effectors differs by 1 order of magnitude according to different investigating methods.[38] Thus, it was confirmed that a BZF molecule also binds selectively to one α subunit under not only a crystalline state, but also a solution state.

The dissociation constant, 1.6 × 10^{-1} M, between BZF and HbA in the fully liganded form is larger than those between BPG and IHP and HbA in deoxy form; these constants are 10^{-5}∼10^{-4} M and 10^{-7}∼10^{-6} M, respectively,[38] which suggests that the style of interaction between BZF and HbA in the fully liganded form is different from that between BPG (or IHP) and HbA in deoxy form, judging from the values of the dissociation constants.

pH Dependence of the Strength of BZF Binding to Hbs. To investigate the binding site of BZF to HbA in the fully liganded form we observed paramagnetically shifted heme methyl proton signals of met-azido HbA under various values of pH in the absence or presence of BZF. The low-field portion of the 400 MHz ^{1}H NMR spectra of met-azido HbA in the absence or presence of BZF at different values of pH at 45 °C is illustrated in the spectra (see Figures SI 1 and SI 2). The differences ($\Delta\delta$) of chemical shifts—subtracting chemical shifts in the absence of BZF from chemical shifts in the presence of BZF—were calculated for the various pH values.

Figure 3 shows the $\Delta\delta$ of 12- and 18-Me proton signals in the α subunit against the various pH values (δ−pH plots). The $\Delta\delta$

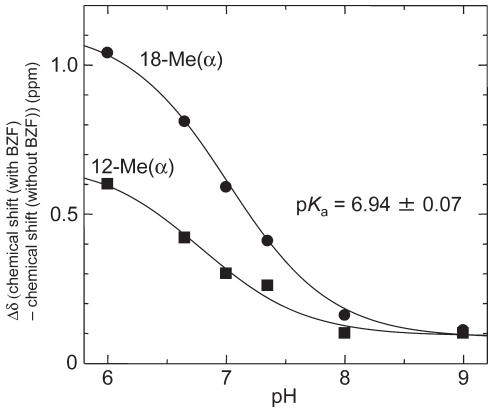

Figure 3. The pH dependence of the different chemical shifts between heme methyl proton signals of the 400 MHz ^{1}H NMR spectra of met-azido HbA at 45 °C in the absence of BZF and in the presence of [BZF]/[heme] of 40. The different chemical shifts of the α subunit are shown in closed symbols: 12-Me (square: ■) and 18-Me (circle: ●).

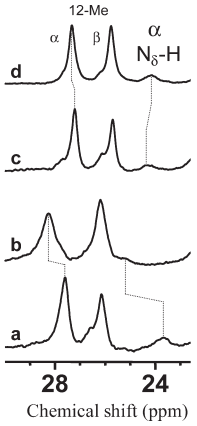

Figure 4. 400 MHz ^{1}H NMR spectra of met-azido HbA at 35 °C in the absence of BZF at pH 6.0 (a) and pH 8.0 (c) and in the presence of [BZF]/[heme] of 40 at pH 6.0 (b) and pH 8.0 (d).

of 12- and 18-Me proton signals in α subunit are observed clearly below pH 8.0 (see Figures SI 1 and SI 2). The δ−pH plots were fitted by the Hasselbalch equation. The pK_a value was calculated as 6.94 ± 0.07 from the $\Delta\delta$ of 18-Me proton and 12-Me proton in the α subunit. The change of chemical shift of 2-Me proton in the α subunit against pH is too small to allow for calculation of the pK_a value (see Figure SI 3). The pK_a value reflects the electronic structure change of heme methyl proton in the α subunit through interaction between BZF and amino acid residue in the α subunit. Because carboxylic acid of BZF remains deprotonated (ref 39 and see Figure SI.4) in the investigated pH range (pH 6 to 9), the pK_a value is attributable to protonation/deprotonation of amino acid residue in the α subunit.

The low-field portion of the 400 MHz ^{1}H NMR spectra of met-azido HbA at various pH values and in the absence or presence of BZF was recorded (Figure 4, and see Figure SI 5) to investigate the property of the coordination bond between proximal histidine and heme. Figure 4 shows 12-Me proton signals in the α subunit of met-azido HbA in the absence or presence of BZF at pH 6.0 and 8.0 at 35 °C. Each peak observed near 24 ppm in the absence of BZF is proximal N_δ-H proton of the α subunit. These peaks exhibited downfield-shifted and line-broadening heme methyl proton signals caused by BZF addition, except at pH 8.0. The observations of downfield-shifted and line-broadening heme methyl proton signals of 12-, 2-, 18-Me and of the downfield-shifted proximal HisF8 N_δ-H proton signal of the α subunit suggest an increase of the unpaired electron density of the heme iron of the α subunit and, accordingly, the weakness of the axial ligand field in the heme of the α subunit.

However, it has been reported that a lower pH of the HbA solution in the presence of BZF leads to a larger BZF effect on the reduction of oxygen affinity.[9] This suggests strongly that interaction between BZF and amino acid residue in the α subunit in a low pH environment causes a reduction of oxygen affinity.

■ DISCUSSION

Elongation of the Fe−His Bond in the *α* Subunit Induced upon BZF Binding to the Fully Liganded Form of Hbs. The met-azido derivatives of heme proteins in general share the property in which they exhibit a thermal equilibrium between the high spin, $S = 5/2$, and low spin, $S = 1/2$, state due to the intermediate ligand field strength of the azido ligand.[29−32] Hence, changes in the population of the two spin states in equilibrium provide a sensitive probe of the effective axial field strength. Both the spectral pattern of heme methyl protons (Figure 2) and of proximal N_δ−H proton (Figure 4) clearly show that upon BZF addition, the shifts for the heme methyl protons and proximal N_δ−H proton increase for the heme of the α subunit. Thus, the position of the spin equilibrium upon BZF addition moves to a higher spin for the heme of the α subunit.

The shift of the spin equilibrium observed in the α subunit can be considered as follows. One case is the elongation of the Fe−His (proximal HisF8) bond. The other case is the elongation of the Fe−N (N_3^-) bond between Fe and N_3^-, which is an exogenous ligand. Many paramagnetic ^{1}H NMR studies of HbA and related compounds in met-azido form indicate that the more extensive population at the high spin state reflects primarily the effective ligand field of the ligand trans to the bound-azido ion, i.e., the Fe−His (proximal HisF8) bond.[40,41] Moreover, in a previous resonance Raman study, Fe−CO frequencies in COHb with and without BZF are the same.[26] This suggests that the BZF binding to the fully liganded form does not affect the Fe-ligand bond. Therefore, the shift of thermal spin equilibrium in the α subunit upon BZF addition is considered as the elongation of the Fe−His bond.

The elongation of the Fe−His bond from the α subunit of HbA upon the binding of BZF to the protein is consistent with the reduction of Fe−His stretching frequency after CO photodissociation of COHb in the presence of BZF.[26] The observed Fe−His frequency after 10 ps CO photodissociation of COHb is 231 cm^{-1} and 229 cm^{-1}, in the absence and presence, respectively, of BZF. Friedman et al. report that Fe−His frequencies after 8 ns CO photodissociation of COHb decrease in the presence of allosteric effectors.[21−25] The slight low frequency shift due to BZF addition shows the elongation of the Fe−His bond in the α or β subunit of the fully liganded form (COHb).[26] Considering that both met-azido HbA and COHb, which are fully liganded forms, adopt the R quaternary structure,[33] it is strongly suggested that the tertiary structure change of Hbs induced by the binding of BZF to the fully liganded form of Hbs causes the elongation of Fe−His in the α subunit. Our conclusion is supported by the molecular dynamics (MD) calculation of

Yonetani and Laberage.[42] In their MD calculation, the main chain of HbA fluctuated more in the presence of BZF than in the absence of BZF. In particular, the main chain in E and F helices fluctuates largely, and the fluctuation extends the distances between Fe and distal Histidine (HisE7) and between Fe and proximal Histidine (HisF8). This increased fluctuation in the E and F helices results in weakness of the Fe−His bond.

Relation between the Elongation of the Fe−His Bond in the α Subunit and Oxygen Affinity. The elongation of the Fe−His bond is also confirmed in the quaternary structure change.[27,43] In the quaternary structure of R and T of HbA and related Hbs in deoxy form, Fe−His frequencies are observed at 223 cm^{-1} and 203 cm^{-1} for the α subunit and at 224 cm^{-1} and 217 cm^{-1} for the β subunit.[27,43] The elongation of the Fe−His bond concomitant with the quaternary structure change from R to T results in a decrease of oxygen affinity.[27,44] Thus, it was suggested that the elongation of the Fe−His bond caused by not only the quaternary structure change but also the tertiary structure change is important in the regulation of oxygen affinity.

Moreover, Capece et al. reported that the elongation of the Fe−His bond leads to a reduction of oxygen affinity based on a quantum mechanics calculation.[45] In their quantum mechanics calculation, they characterized the proximal affinity regulation mechanism operative in heme proteins by means of a density functional theory calculation on porphyrin model systems. They analyzed the three main factors controlling proximal regulation: the charge relay mechanism, the proximal histidine rotational position, and the distance between the proximal histidine and the Fe atom.

They believe that the strength of the Fe−His bond is an indicator of the degree of charge donation from His to the iron, and that the increase of the negative charge of the heme iron atom through the strong Fe−His leads the efficient π-back-donation, and therefore makes the dioxygen more negative and increases the strength of Fe−O bonds. Moreover, similar results are reported in regards to the decrease of the negative charge of the heme iron atom upon the introduction of an electron-withdrawing CF_3 (perfluoromethyl) group(s).[46] Thus, it has been experimentally and theoretically demonstrated that the elongation of the Fe−His bond leads to a reduction of oxygen affinity.

Binding Site of BZF to Fully Liganded Form of Hbs. Figures 2, 3, and 4 suggest that BZF interacts with α subunits, and our result is apparently consistent with the previous finding, based on X-ray crystallography, that BZF binds to the α heme in the CO form of horse Hb.[14] However, Shibayama et al. indicate that BZF binds on E-helices and that the binding styles of BZF are both the hydrophobic interaction between chlorine atoms of BZF and carbon atoms of AlaE14, E17, F1, and F4 and the hydrogen bond among nitrogen and oxygen atoms of BZF, H_2O, and AspE13 and LysE10.[14] It seems to be difficult to bind the BZF to the fully liganded form of horse Hb with the hydrogen bond that includes H_2O under the solution. Moreover, in that binding site (E-helix),[14] the pH dependence of the binding strength in the BZF binding to the fully liganded form cannot be interpreted. The homology between horse HbA and human Hb (HbA) is 72%.[47] The amino acid residues near the heme are almost the same. This suggests that the binding site of BZF under the solution is different from that of the crystalline state in horse Hb.

Analysis of the pH dependence of heme methyl proton signals in the presence of BZF provided us with the pK_a value, calculated as 6.94 ± 0.07 (Figure 3). This value is likely to reflect the pK_a value of an amino acid residue, and hence His can be considered to be a candidate.[48]

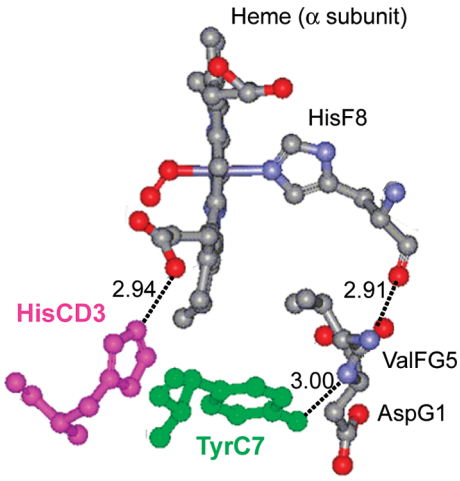

Figure 5. The molecular structure around heme and of amino acids interacting with BZF. (PDB: 1IRD).

In swMb and horse Mb Cocco et al. assigned the pK_a of His imidazole side chains.[49] The range of pK_a of His in swMb is between 5.37 and 8.18. Cocco et al. reported that the relatively high pK_a values (7.84 and 8.18) observed in His 36 of swMb and horse Mb, respectively, are presumably due in part to interaction with Glu 38.[49] Thus, the negatively charged carboxylate of Glu stabilizes the protonated imidazole (imidazolium) of His and so increases the pK_a of His 36 to a value that is higher than the pK_a (6.04) of free His. In the present study, the N_ε atom of HisCD3 in the α subunit is 2.94 Å with O atom of 13-propionate of heme. This distance would be enough to stabilize protonated imidazole of HisCD3 and so the pK_a of imidazole of HisCD3 seems to increase more than does the pK_a (6.04) of free His.

Regarding determination of the binding site of BZF, it is very important to consider the distance between heme and His interacting with BZF, because we observe the heme electronic structure change through the structure change of His due to the binding of BZF. HisCD3 has the shortest distance between Fe and C_ε, 12.10 Å, of the eight Histidines of the α subunit, except for proximal and distal Histidines. This short distance (12.10 Å) between HisCD3 (C_ε) and the heme iron atom would make possible the electronic structure change of heme caused by the perturbation of HisCD3 residue.[50] When we consider BZF concentration dependence in met-azido HbA solution at pH 7.0 (Figure 2), the difference of chemical shifts between the absence and presence of BZF in heme methyl proton increases more in 12- and 18-Me than in 2-Me. According to X-ray crystallography of COHb (PDB:1IRD),[50] HisCD3 forms a hydrogen bond with 13-propionate of heme in the α subunit. The distance between N_ε of HisCD3 and the O atom of 13-propionate is 2.72 Å. A carboxylate of BZF may form the hydrogen bond with protonated HisCD3. The electronic structure change of 13-propionate due to the interaction with carboxylate of BZF may influence the electronic structure of 12- and 18-Me more effectively than it influences that of 2-Me.

Moreover, if BZF interacts with HisCD3 in the α subunit, a benzene ring of TyrC7 near HisCD3 may interact with the terminal benzene ring of BZF through $\pi-\pi$ stacking interaction.

TyrC7 perturbed by the interaction with the benzene ring of BZF binding may also influence the paramagnetically shifted ^{1}H signal of 12-Me through the close distance (3.73 Å) between C_β of TyrC7 and C_α of 12-Me. Thus, the down-fielded chemical shift measured in the α heme (but not the β and γ heme) methyl proton signals in met-azido HbA and HbF caused by BZF addition can be interpreted as the interaction between BZF and HisCD3 or TyrC7.

Mechanism of Elongation of Fe−His Bond in the α Subunit Due to the Binding of BZF to the Fully Liganded Form. In the mechanism of the elongation of the Fe−His bond in the α subunit, it is supposed that when BZF interacts with HisCD3 and TyrC7 in the α subunit, the interaction causes the movement of F-helix and the FG corner through hydrogen bond networks between TyrC7 and AspG1 and between HisF8 and ValFG5, which is covalently connected with AspG1 by a peptide bond.

The distance of the hydrogen bond is 3.00 and 2.91 Å for (TyrC7 O_η---AspG1 N (main chain)) and (ValFG5 N (main chain)---HisF8 O (main chain)), respectively. This distance of hydrogen bond is not so weak in the hydrogen bond of N---O type.[51] The elongation of the Fe−His bond in the α subunit is reflected in the down-shifted N_δ−H and heme methyl proton signals and in the increase of the line width of the heme methyl proton signals in the α subunit. Figure 5 shows plausible interactions among HisCD3, TyrC7, and BZF.

CONCLUSIONS

The present study demonstrated that the binding of BZF to met-azido HbA resulted in a slight elongation of the Fe−His bond that occurred selectively in the α subunit. Considering the fact that the Fe−His bond of the α subunit in low oxygen affinity T state is longer than that in the high-oxygen affinity R state, the detected elongation of the Fe−His bond reasonably accounts for the reduction of the oxygen affinity of HbA in the presence of BZF. It was suggested that the elongation of the Fe−His bond, which causes not only quaternary structure change but also tertiary structure change, plays an important role in the regulation of oxygen affinity.

Regarding the mechanism of the elongation of the Fe−His bond in the α subunit, it was supposed that when BZF interacts with HisCD3 and TyrC7 in the α subunit, the interaction causes the movement of F-helix and the FG corner through hydrogen bond networks between TyrC7 and AspG1 and between HisF8 and ValFG5, which is covalently connected with AspG1 by a peptide bond.

ASSOCIATED CONTENT

Supporting Information. Title: elongation of the Fe−His bond in the α subunit induced by binding of the allosteric effector bezafibrate to hemoglobins. Authors: Shigenori Nagatomo, Hiromi Hamada, and Hiroyuki Yoshikawa. SI 1−5 (PDF), 5 pages. This material is available free of charge via the Internet at http://pubs.acs.org.

AUTHOR INFORMATION

Corresponding Author

*Phone: +81-29-853-5768; Fax: +81-29-853-6503; E-mail: nagatomo@chem.tsukuba.ac.jp.

ACKNOWLEDGMENT

We thank Professor Yasuhiko Yamamoto for helpful suggestions regarding the preparation of the manuscript.

ABBREVIATIONS USED

HbA, human adult hemoglobin; HbF, human fetal hemoglobin; CO, carbon monoxide; COHb, carbonmonoxy hemoglobin; Me, methyl group; CF_3, perfluoromethyl; BPG, 2,3-bisphosphoglycerate; IHP, inositol(hexakis)phosphate; BZF, bezafibrate

REFERENCES

(1) Monod, J.; Wyman, J.; Changeux, J. P. *J. Mol. Biol.* **1965**, *12*, 88–118.
(2) Arnone, A. *Nature* **1972**, *237*, 146–149.
(3) Benesch, R.; Benesch, R. E. *Biochem. Biophys. Res. Commun.* **1967**, *26*, 162–167.
(4) Perutz, M. F. *Nature* **1970**, *228*, 726–739.
(5) Perutz, M. F. *Annu. Rev. Biochem.* **1979**, *48*, 327–386.
(6) Perutz, M. F. *Annu. Rev. Physiol.* **1990**, *52*, 1–25.
(7) Perutz, M. F.; Fermi, G.; Luisi, B.; Shaanan, B.; Liddington, R. C. *Acc. Chem. Res.* **1987**, *20*, 309–321.
(8) Shulman, R. G.; Hopfield, J. J.; Ogawa, S. *Q. Ann. Rev. Biophys.* **1975**, *8*, 325–420.
(9) Yonetani, T.; Park, S. I.; Tsuneshige, A.; Imai, K.; Kanaori, K. *J. Biol. Chem.* **2002**, *277*, 34508–34520.
(10) Tsuneshige, A.; Park, S. I.; Yonetani, T. *Biophys. Chem.* **2002**, *98*, 49–63.
(11) Perutz, M. F.; Poyart, C. *Lancet* **1983**, *2*, 881–882.
(12) Perutz, M. F.; Fermi, G.; Abraham, D. J.; Poyart, C.; Bursaux, E. *J. Am. Chem. Soc.* **1986**, *108*, 1064–1078.
(13) Lalezari, I.; Lalezari, P.; Poyart, C.; Marden, M.; Kister, J.; Bohn, B.; Fermi, G.; Perutz, M. F. *Biochemistry* **1990**, *29*, 1515–1523.
(14) Shibayama, N.; Miura, S.; Tame, R. H. J.; Yonetani, T.; Park, S.-Y. *J. Biol. Chem.* **2002**, *277*, 38791–38796.
(15) Friedman, J. M.; Scott, T. W.; Stepnoski, R. A.; Ikeda-Saito, M.; Yonetani, T. *J. Biol. Chem.* **1983**, *258*, 10564–10572.
(16) Friedman, J. M.; Scott, T. W.; Fisanick, G. J.; Simon, S. R.; Findsen, E. W.; Ondrias, M. R.; Macdonald, V. W. *Science* **1985**, *229*, 187–190.
(17) Scott, T. W.; Friedman, J. M.; Macdonald, V. W. *J. Am. Chem. Soc.* **1985**, *107*, 3702–3705.
(18) Jayaraman, V.; Rodgers, K. R.; Mukerji, I.; Spiro, T. G. *Science* **1995**, *269*, 1843–1848.
(19) Hu, X.; Frei, H.; Spiro, T. G. *Biochemistry* **1996**, *35*, 13001–13005.
(20) Peterson, E. S.; Friedman, J. M. *Biochemistry* **1998**, *37*, 4346–4357.
(21) Huang, J.; Juszczak, L. J.; Peterson, E. S.; Shannon, C. F.; Yang, M.; Huang, S.; Vidugiris, G. V. A.; Friedman, J. M. *Biochemistry* **1999**, *38*, 4514–4525.
(22) Samuni, U.; Juszczak, L.; Dantsker, D.; Khan, I.; Friedman, A. J.; Perez-Gonzalez-de-Apodaca, J.; Bruno, S.; Hui, H. L.; Golby, J. E.; Karasik, E.; et al. *Biochemistry* **2003**, *42*, 8272–8288.
(23) Peterson, E. S.; Shinder, R.; Khan, I.; Juczszak, L.; Wang, J.; Manjula, B.; Acharya, S. A.; Bonaventura, C.; Friedman, J. M. *Biochemistry* **2004**, *43*, 4832–4843.
(24) Samuni, U.; Dantsker, D.; Juszczak, L. J.; Bettati, S.; Ronda, L.; Mozzarelli, A.; Friedman, J. M. *Biochemistry* **2004**, *43*, 13674–13682.
(25) Samuni, U.; Roche, C. J.; Dantsker, D.; Juszczak, L.; Friedman, J. M. *Biochemistry* **2006**, *45*, 2820–2835.
(26) Nagatomo, S.; Nagai, M.; Mizutani, Y.; Yonetani, T.; Kitagawa, T. *Biophys. J.* **2005**, *89*, 1203–1213.
(27) Kitagawa, T. Biological Applications of Raman Spectroscopy. In *Biological Applications of Raman Spectroscopy, Vol.* 3; Spiro, T. G., Ed.; John Wiley & Sons: New York, 1988; pp 97−131.

(28) Mizutani, Y.; Nagai, M. *Chem. Phys.* DOI: 10.1016/j.chemphys.2011.05.012.
(29) Iizuka, T.; Morishima, I. *Biochim. Biophys. Acta* **1974**, *371*, 1–13.
(30) La Mar, G. N.; Y. Yamamoto, Y.; Jue, T.; Smith, K. M.; Pandey, R. K. *Biochemistry* **1985**, *24*, 3825–3831.
(31) Yamamoto, Y.; La Mar, G. N. *Biochemistry* **1986**, *25*, 5288–5297.
(32) Yamamoto, Y.; Nagaoka, T. *FEBS* **1998**, *424*, 169–172.
(33) Perutz, M. F.; Fersht, A. R.; Simon, S. R.; Roberts, G. C. K. *Biochemistry* **1974**, *13*, 2174–2186.
(34) Nagai, K.; Hori, H.; Morimoto, H.; Hayashi, A.; Taketa, F. *Biochemistry* **1979**, *18*, 1304–1308.
(35) Prins, H. K. *J. Chromatogr.* **1959**, *2*, 445–486.
(36) Coletta, M.; Angeletti, M.; Ascenzi, P.; Bertollini, A.; Longa, S. D.; De Sanctis, G.; Priori, A. M.; Santucci, R.; Amiconi, G. *J. Biol. Chem.* **1999**, *274*, 6865–6874.
(37) Ascenzi, P.; Bertollini, A.; Coletta, M.; Desideri, A.; Giardina, B.; Polizio, F.; Santucci, R.; Scatena, R.; Amiconi, G. *J. Inorg. Biochem.* **1993**, *50*, 263–272.
(38) Imai, K. *Allosteric Effects in Haemoglobin*; Cambridge University Press: Cambridge, UK, 1982; pp 43−44.
(39) Lindqvist, N.; Tuhkanen, T; Kronberg, L. *Water Res.* **2005**, *39*, 2219–2228.
(40) Yamamoto, Y.; La Mar, G. N. *Biochim. Biophys. Acta* **1989**, *996*, 187–194.
(41) Morishima, I.; S. Neya, S.; Inubushi, T.; Yonezawa, T.; IIzuka, T. *Biochim. Biophys. Acta* **1978**, *534*, 307–316.
(42) Yonetani, T.; Laberge, M. *Biochim. Biophys. Acta* **2008**, *1784*, 1146–1158.
(43) Nagai, K.; Kitagawa, T. *Proc. Natl. Acad. Sci. U.S.A.* **1980**, *77*, 2033–2037.
(44) Matsukawa, S.; Mawatari, K.; Yoneyama, Y.; Kitagawa, T. *J. Am. Chem. Soc.* **1985**, *107*, 1108–1113.
(45) Capece, L.; Marti, M. A.; Crespo, A.; Doctorovich, F.; Estrin, D. A. *J. Am. Chem. Soc.* **2006**, *128*, 12455–12461.
(46) Shibata, T.; Nagao, S.; Fukaya, M.; Tai, H.; Nagatomo, S.; Morihashi, K.; Matsuo, T.; Hirota, S.; Suzuki, A.; Imai, K.; et al. *J. Am. Chem. Soc.* **2010**, *132*, 6091–6098.
(47) Dickerson, R. E.; Geis, I. *Hemoglobin: Structure, Function, Evolution, and Pathology*; Benjamin Cummings: Menlo Park, 1983; p 32.
(48) Dawson, R. M. C.; Elliott, W. H.; Jones, K. M. *Data for Biochemical Research*, 3rd ed.; Oxford Science Publications: New York, 1986; pp 1−31.
(49) Cocco, M. J.; Kao, Y.-H.; Phillips, A. T.; Lecomte, T. J. *Biochemistry* **1992**, *31*, 6481–6491.
(50) Park, S.-Y.; Tame, J. R. H. Crystal Structure of Human Carbonmonoxy-haemoglobin at 1.25 Å Resolution, 2003 (PDB: 1IRD).
(51) Pimentel, G. C.; McClellan, A. L. *The Hydrogen Bond*. Drawings by Roger Hayward. Freeman: San Francisco, 1960; p 289.